Framework for Determining Lateral Minimum Separation Distance Using ADS-B Information

Junsoo Kim, Gihun Nam, Jiyun Lee
Korean Advanced Institute of Science and Technology

Dongchan Min, Sam Pullen
Stanford University

ABSTRACT

Urban air mobility (UAM) is expected to increase traffic density in constrained low-altitude airspace, thereby increasing the risk of mid-air collisions and emphasizing the need for safe yet efficient separation management. Conventional aviation separation standards are too large to be directly applied to UAM without severely reducing airspace efficiency. Our prior research introduced a safety risk assessment (SRA)-based methodology for determining the minimum separation distance (MSD) for UAM tactical deconfliction. However, the earlier framework relied on a generic surrogate detection model and was limited to nominal operation. This study extends the framework by introducing an Automatic Dependent Surveillance-Broadcast (ADS-B)-based representation of tactical deconfliction and by explicitly accounting for identified failure conditions in both the navigation system and the detection system. In the proposed approach, ADS-B integrity parameters, including the navigation integrity category (NIC), source integrity level (SIL), and source design assurance (SDA), are used to model traffic-state uncertainty, detection uncertainty, and ADS-B failure probability in a direct and traceable manner. Navigation-system failure conditions are represented as biases in the ownship total system error (TSE), while ADS-B failure conditions are modeled by loss of detection capability. A case study was conducted for a UAM system equipped with a GNSS/INS-integrated extended Kalman filter navigation system and an ADS-B-based detection system. The proposed methodology was used to compute the MSD and to analyze its sensitivity to ADS-B integrity parameters and ownship navigation system configurations. The results show that improving ADS-B integrity can substantially reduce the required separation distance. In particular, when NIC is improved from 8 to 9 and SDA is improved from 2 to 3, the final MSD decreases from 128 m to 88 m, achieving up to a 31% reduction. In addition, among the ownship navigation configurations considered, the dual-frequency multi-constellation configuration yields the smallest MSD, indicating that it is the most effective for reducing separation requirements while maintaining the required level of safety.

Keywords: urban air mobility, minimum separation distance, safety risk assessment, automatic dependent surveillance-broadcast, tactical deconfliction

1.0 INTRODUCTION

The rapid expansion of urban air mobility (UAM) and unmanned aerial systems (UASs) operations is expected to significantly increase aircraft density in low-altitude urban airspace. This increased density elevates the risk of airborne collisions, making safe separation between aircraft a primary safety concern [1]. Current aviation practices employ substantial separation standards (e.g., 5 nautical miles horizontally and 2,000 feet vertically), which, if applied directly to UAM and UAS operations, would severely hinder airspace capacity [2]. Therefore, accommodating this anticipated growth within constrained urban airspaces necessitates a reduction in separation standards. Any reduction, however, inherently increases collision risk and must be rigorously validated to ensure compliance with the target level of safety (TLS).

Several established methodologies have been developed to reduce separation standards required to meet the TLS. The reduced vertical separation minimum (RVSM) protocol represents the conventional approach in manned aviation, in which extensive operational data are analyzed to assess mid-air collision (MAC) and near mid-air collision (NMAC) rates under reduced vertical separation (e.g., from 2,000 to 1,000 feet vertically) [2]. In parallel, UAS researchers have employed high-fidelity simulations to evaluate MAC and NMAC rates for candidate well clear volume dimensions, which define separation criteria between UAS and manned aircraft [3]. These approaches have contributed to certification and pre-implementation assessments through

rigorous statistical analysis. However, both rely on post-processed flight data or large-scale simulations, limiting their applicability to UAM and UAS operations, for which operational flight data remain scarce [4].

To address this challenge, our prior work [4-6] proposed a systematic approach for determining minimum separation distance (MSD) with reduced reliance on operational flight data. Specifically, we introduced a safety risk assessment (SRA) framework to derive the lateral MSD that satisfies the TLS. The framework models both strategic and tactical deconfliction through a detect-and-avoid (DAA) system, which serves as a procedural means of preventing potential collisions in UAM and UAS operations. However, the initial framework had three key assumptions. First, in the absence of traffic state information, surrounding traffic was assumed to occupy the worst-case encounter geometry, and its navigation performance was assumed to correspond to the worst-performing system authorized in the airspace. Second, the DAA system was represented by a generic surrogate model characterized by a single uncertainty parameter, which lacked a direct mapping to actual system specifications. Third, the analysis was limited to nominal operation, and sensor failure conditions were not accounted for, although such failures can become significant contributors to collision risk under a stringent TLS. While these assumptions simplified the MSD evaluation and provided a conservative basis for nominal operation, they resulted in overly large MSDs applicable only to the nominal condition.

This study addresses these limitations by introducing an automatic dependent surveillance-broadcast (ADS-B)-based representation of tactical deconfliction into the SRA framework. ADS-B periodically broadcasts aircraft state information together with accuracy and integrity indicators, and it is already widely used in aviation surveillance and DAA applications [7]. This makes ADS-B a practical basis for replacing the previous surrogate detection model and relaxing part of the conservative traffic assumptions. In the SRA, collision risk is evaluated from three linked events: separation violation, detection failure, and collision. ADS-B improves the last two terms in a direct and traceable way. First, ADS-B integrity information such as the navigation integrity category (NIC) and source integrity level (SIL) is introduced to characterize both the traffic state information and navigation performance. Second, the previously generic detection model is replaced with a concrete ADS-B-based model, in which the detection uncertainty is explicitly represented using ADS-B characteristics and integrity parameters, thereby making the model more physically interpretable and more directly linked to actual system specifications.

In addition, the framework is extended to sensor-failure conditions in both the navigation system and the detection system, thereby addressing the third limitation of the prior work. Navigation-system failures are modeled as biases in the ownship total system error (TSE) distribution, because such failures could displace the estimated ownship position and thereby increase collision risk. In contrast, detection-system failures are modeled through ADS-B failure conditions represented by the source design assurance (SDA), which determines the prior probability of ADS-B malfunction. Under such conditions, the ADS-B-based detection system is treated as unavailable, and the associated collision risk is evaluated without crediting tactical detection. By explicitly accounting for the identified failure cases in both the navigation and detection systems, including ADS-B failure, the proposed analysis is no longer limited to nominal operation. As a result, the method becomes more robust and more reliable for stringent safety requirements and for practical UAM operations.

To demonstrate the proposed methodology, we conduct a case study using a GNSS/INS-integrated navigation system and an ADS-B-based detection system. The case study applies the proposed framework to compute the lateral MSD and then examines its sensitivity to ADS-B integrity parameters, particularly NIC, SIL and SDA. In addition, we evaluate several ownship navigation configurations by comparing the MSDs obtained with different GNSS and IMU combinations. This analysis shows how both ADS-B integrity performance and ownship navigation performance affect the final MSD, and it helps identify navigation-system configurations that reduce MSD more effectively while maintaining the required level of safety.

The remainder of this paper is organized as follows. Section 2 provides the background on strategic and tactical deconfliction and the safety-assured MSD. Section 3 introduces ADS-B and its integrity information. Section 4 presents the proposed framework for determining the lateral minimum separation distance using ADS-B information. Section 5 describes the case study and discusses the results. Finally, Section 6 concludes the paper.

2.0 Background

This section provides background on deconfliction concepts relevant to UAM operations. It reviews strategic and tactical deconfliction within deconfliction barriers and summarizes a safety-assured approach for determining the MSD.

2.1 Strategic and Tactical Deconfliction

Figure 1 illustrates the deconfliction barriers commonly adopted for UAS and UAM operations, consisting of the Well Clear Threshold (WCT), Well Clear Volume (WCV), Collision Avoidance Threshold (CAT), and Collision Volume (CV) [8, 9]. Based on these barriers, deconfliction can be classified into strategic and tactical layers.

Strategic deconfliction operates at longer time horizons through pre-flight planning or long-term trajectory monitoring. It aims to prevent conflicts by adjusting routes or times of arrival [8]. In this layer, safety is ensured through predefined paths that are determined prior to flight and remain unchanged during operation [9]. Separation is maintained by ensuring that the WCVs of aircraft do not overlap. When only strategic deconfliction is available, the separation distance (SD) is defined by the size of the WCV; the extent of the WCV along the relevant axis corresponds directly to the SD used for separation assurance.

Tactical deconfliction provides an additional protective layer by monitoring intruders at shorter time scales (e.g., up to 30 minutes) and executing mild avoidance maneuvers before the WCV is penetrated [8]. As shown in Figure 1, the introduction of tactical deconfliction establishes an outer activation region, referred to as the WCT, which protects the WCV from intrusion [8]. Consequently, when tactical deconfliction is available, the SD is defined by the extent of the WCT rather than by the WCV itself. In this study, which focuses on one-dimensional (1-D) lateral separation, the lateral extent of the WCT is defined as the SD. Note that, although tactical deconfliction introduces an additional boundary, the resulting reduction in collision risk allows a smaller SD to satisfy the same safety requirement [5, 6].

Collision avoidance serves as the last line of defense and is activated only after the CAT is violated [8]. This layer relies on aggressive maneuvers, such as abrupt climbs or descents, to avoid imminent collisions. Systems such as traffic collision avoidance system (TCAS) exemplify this layer [9]; however, collision avoidance is not considered a separation management function in this work.

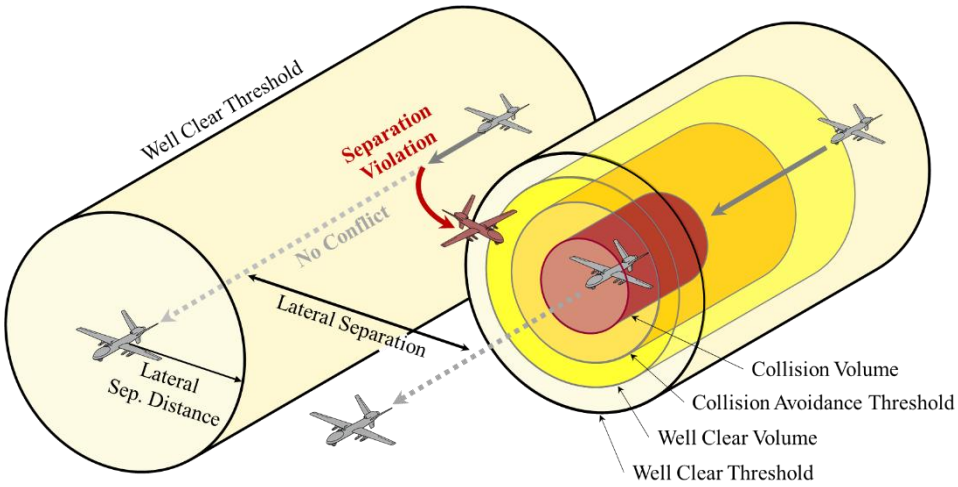

FIGURE 1 Lateral Separation Scenario and Deconfliction Barriers for UAS and UAM Operations.

2.2 Safety Assured Minimum Separation Distance

In our prior work, we introduced the concept of the MSD as the smallest separation distance that satisfies a prescribed TLS for UAM operations [4-6]. The MSD is derived using an SRA framework that explicitly relates SD to collision risk. An overview of the framework is shown in Figure 1 of [4]. The SRA begins by allocating the system-level TLS to the relevant subsystem. This allocated TLS is then converted into an allowable separation violation (SV) probability requirement, denoted as $P_{SV,REQ}$, by dividing the allocated TLS by the fatality-to-SV ratio [4]. The MSD is determined as the SD at which the probability of SV equals $P_{SV,REQ}$.

The probability of SV is determined based on the TSE distribution, which is the root-sum-square (RSS) of navigation system error (NSE) and flight technical error (FTE). In addition, both strategic and tactical deconfliction are reflected in the SRA structure [5-6]. Strategic deconfliction reduces the probability of SV through pre-flight path planning, while tactical deconfliction further mitigates collision risk by enabling DAA actions after an SV occurs. When tactical deconfliction is implemented, the fatality-to-SV ratio decreases, resulting in a larger $P_{SV,REQ}$ and consequently a smaller MSD.

The MSD framework was developed as a pre-implementation assessment methodology based on system-level safety and performance analysis [4–6]. A key advantage of this framework is that it reduces dependence on extensive operational flight data by deriving the required separation distance from system specifications, performance models, and conservative operational assumptions. This feature makes the framework well suited to the early stages of UAM deployment, where representative operational data are scarce but safety-driven separation requirements must still be established.

3.0 ADS-B and Baseline UAM System Configuration

ADS-B is a cooperative surveillance system in which aircraft periodically broadcast GPS-based position, velocity, and related navigation quality information [7]. In addition to accuracy information, ADS-B also provides integrity information, which is particularly useful for safety-critical applications. In this study, ADS-B is introduced as the basis for modeling detection system in the UAM operation. This section describes the ADS-B integrity parameters used in the analysis and then presents the baseline UAM system configuration adopted in this study.

3.1 ADS-B Integrity Parameters

ADS-B broadcasts several standardized parameters that describe the quality of the reported aircraft state. Among them, this study uses three parameters: navigation integrity category (NIC), source integrity level (SIL), and source design assurance (SDA). Under federal aviation administration (FAA) regulation (14 CFR § 91.227) [10], NIC is defined as "*an integrity containment radius around an aircraft's reported position*," SIL as "*the probability of the reported horizontal position exceeding the containment radius defined by the NIC on a per sample or per hour basis*," and SDA as "*the probability of an aircraft malfunction causing false or misleading information to be transmitted.*" The values of NIC, SIL, and SDA used in this study are summarized in Table 1.

NIC, SIL, and SDA are used directly in the SRA. NIC and SIL are used to model the uncertainty of the traffic position reported through ADS-B. Specifically, the standard deviation of the ADS-B-based traffic position error is obtained by dividing the NIC containment radius by the Gaussian multiplier corresponding to the SIL. This quantity is then used to construct the traffic position-error distribution. By contrast, SDA is used to represent the prior probability of ADS-B failure in the SRA.

According to 14 CFR § 91.227, ADS-B systems intended to support separation services must satisfy the following condition:

$$NIC \geq 7 \cap SIL = 3 \cap SDA \geq 2.$$

This study assumes ADS-B systems that satisfy this requirement. Under SIL = 3, the reported position source has an integrity level of 10^{-7}. Therefore, the ADS-B position source is treated as sufficiently reliable for the present analysis. Under this assumption, separate failure cases of the ADS-B position source are not modeled in this study. Instead, the SRA includes ADS-B-related failures represented by SDA.

TABLE 1
ADS-B Accuracy and Integrity Parameters (shaded cells denote values required by FAA) [10].

Value	ADS-B Parameters		
	NIC	**SIL***	**SDA****
0	Rc ≥ 37.04 km (or Unknown)	> 10^{-3} (or Not Available)	> 10^{-3} (or Not Available)
1	Rc < 37.04 km (20 NM)	≤ 10^{-3}	≤ 10^{-3}
2	< 14.816 km (8 NM)	≤ 10^{-5}	≤ 10^{-5}
3	Rc < 7.408 km (4 NM)	≤ 10^{-7}	≤ 10^{-7}
⋮	⋮	*Probability of the reported horizontal position exceeding the radius of containment defined by the NIC without alerting, assuming the avionics has no faults.	**Probability of Undetected Fault Causing the Transmission of False or Misleading Information
7	Rc < 370.4 m (0.2 NM)		
8	Rc < 185.2 m (0.1 NM)		
9	Rc < 75 m		
10	Rc < 25 m		
11	Rc < 7.5 m		

3.2 Baseline Configuration for UAM Operation

Figure 3 shows the baseline UAM system configuration considered in this study. The baseline configuration considered here represents the primary system components relevant to collision risk, and it can be extended to account for other collision-related elements. Among the many onboard functions of a UAM vehicle, we focus on the navigation system and the detection system because these two systems directly affect collision risk in the proposed SRA. For analytical tractability, and to isolate the contribution of each system to the collision-risk calculation, the two systems are first assumed to be functionally and statistically independent. The navigation system is formed by navigation sensors such as GNSS, INS, and barometric sensors, and each identified sensor is considered under both nominal and failure conditions. The detection system is based on ADS-B, and its architecture likewise includes both nominal operation and ADS-B failure conditions.

The effect of the navigation system on collision risk is represented through the TSE distribution. Because navigation errors cause lateral position errors of the ownship, the output of the navigation system is modeled as a TSE distribution, which is then used to calculate the probability of SV. The detection system, in contrast, determines whether surrounding traffic is inside the prescribed separation distance, and this decision is based on relative distance. However, the estimated relative distance is also uncertain. This uncertainty is represented by a relative distance distribution. Because of this uncertainty, there exists a probability that the traffic is actually within the separation distance but the detection system fails to detect it. The relative distance distribution is therefore used to calculate the conditional probability of detection failure given separation violation. These two probabilities, obtained from the navigation and the detection system, are then used in the subsequent SRA to evaluate collision risk.

We acknowledge that some correlation may exist between the navigation system and the detection system in practice, for example through shared environmental effects or common information dependencies. Such coupling is not modeled in the present baseline configuration, because the main objective of this study is to quantify the separate contributions of navigation uncertainty and detection capability to collision risk. A more detailed analysis of cross-system correlation will be addressed in future work.

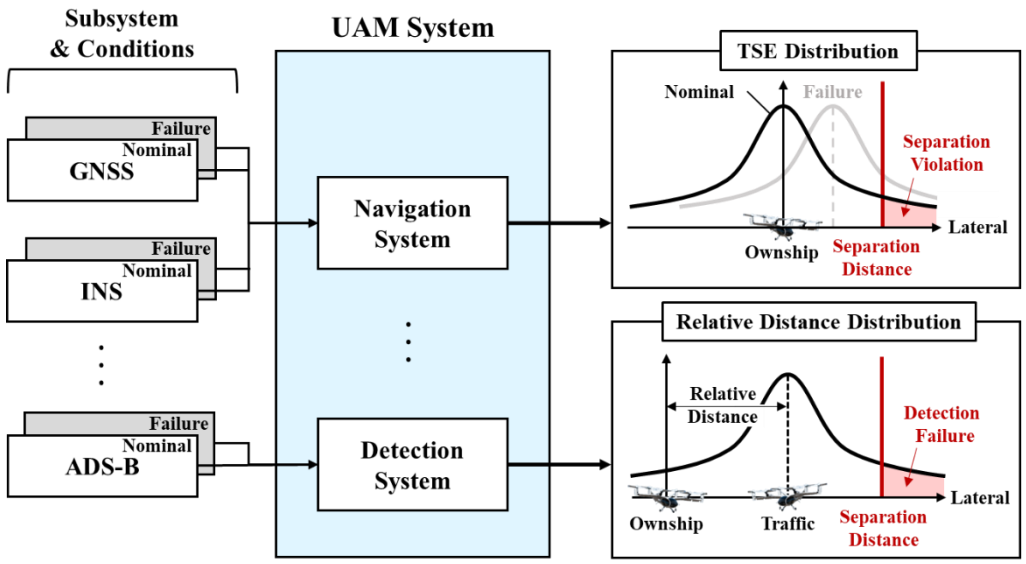

FIGURE 3 Baseline UAM System Configuration. The configuration consists of a navigation system and a detection system, each of which includes nominal and failure conditions. The navigation system produces the TSE distribution for calculating the probability of separation violation, while the detection system produces the relative distance distribution for calculating the probability of detection failure. These probabilities are subsequently used in the SRA to evaluate collision risk.

4.0 Framework for the Minimum Lateral Separation Distance Using ADS-B Information

4.1 Safety Risk Assessment Using ADS-B Integrity Parameters

This section presents an SRA framework for lateral separation based on ADS-B integrity parameters. The analysis focuses on the lateral dimension only; this one-dimensional approach implicitly assumes full overlap in the longitudinal and vertical dimensions, resulting in a conservative estimate of collision risk. The objective of the proposed SRA is to quantify collision risk under tactical deconfliction as an explicit function of separation distance, navigation uncertainty, and detection capability.

Figure 4 provides an overview of the proposed SRA. Once the UAM system configuration is specified, the probability of SV, $P(SV)$, and the probability of detection failure given separation violation, $P(DetF \mid SV)$, can be derived from the navigation and detection system, respectively. These probabilities are then combined with operational assumptions, including the UAM operational scenario, the encounter geometry with the traffic aircraft, and relevant performance requirements, to evaluate the final collision risk. In this framework, $P(CO \mid DetF, SV)$ corresponds to the fatality-to-SV ratio introduced in Section 2.2 and represents the probability that a separation violation followed by a detection failure leads to a collision. Accordingly, this subsection first describes the operational assumptions used in the SRA and then presents the collision risk decomposition and the methods used to compute each probability term.

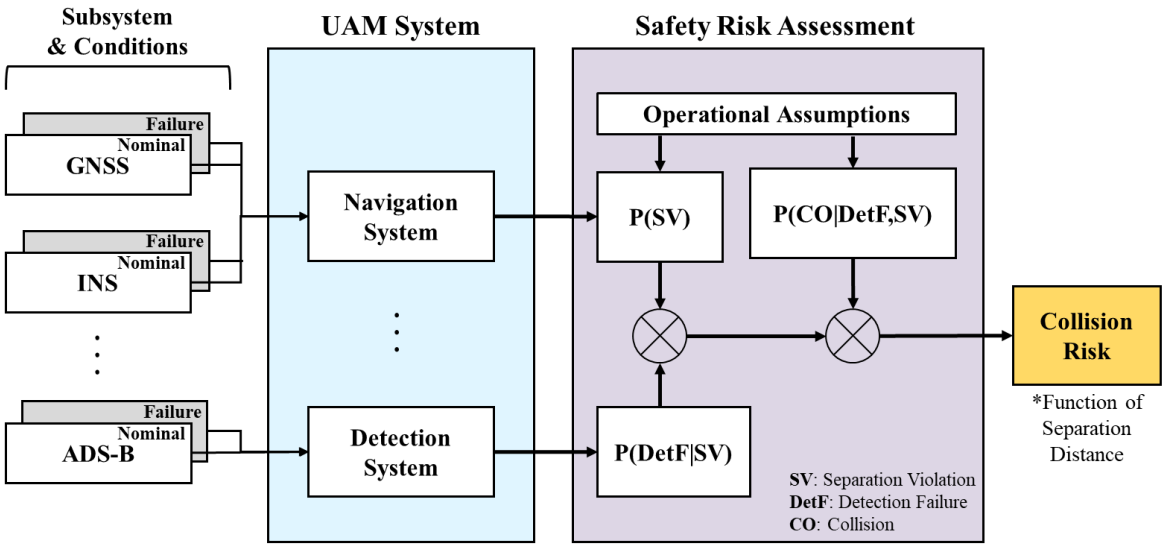

FIGURE 4 Overview of the Safety Risk Assessment.

A. Operational Assumptions

The following operational assumptions are used in the proposed SRA.

First, an SV is defined only from the ownship's perspective. The traffic aircraft is assumed to remain on its planned path and to maintain its assigned separation bound. Therefore, the traffic aircraft does not generate an SV in this framework. Instead, an SV occurs only when the true position of the ownship deviates from the planned path and exceeds the SD. As a result, the probability of SV is determined solely by the ownship's TSE distribution.

Second, the traffic aircraft is assumed to be located at the worst-case encounter geometry. Specifically, it is positioned immediately adjacent to the ownship while still barely maintaining the required SD. This represents the most adverse condition in high-density operation and enables a conservative evaluation even when the actual traffic geometry is not available.

Third, if conflicting traffic is successfully detected, collision is assumed to be avoided. Under this assumption, the proposed framework focuses on the detection function of tactical deconfliction and does not explicitly model the subsequent avoidance maneuver. The effects of avoidance maneuvers, including avoidance logic and maneuver dynamics, are outside the scope of this paper and are being investigated in ongoing work.

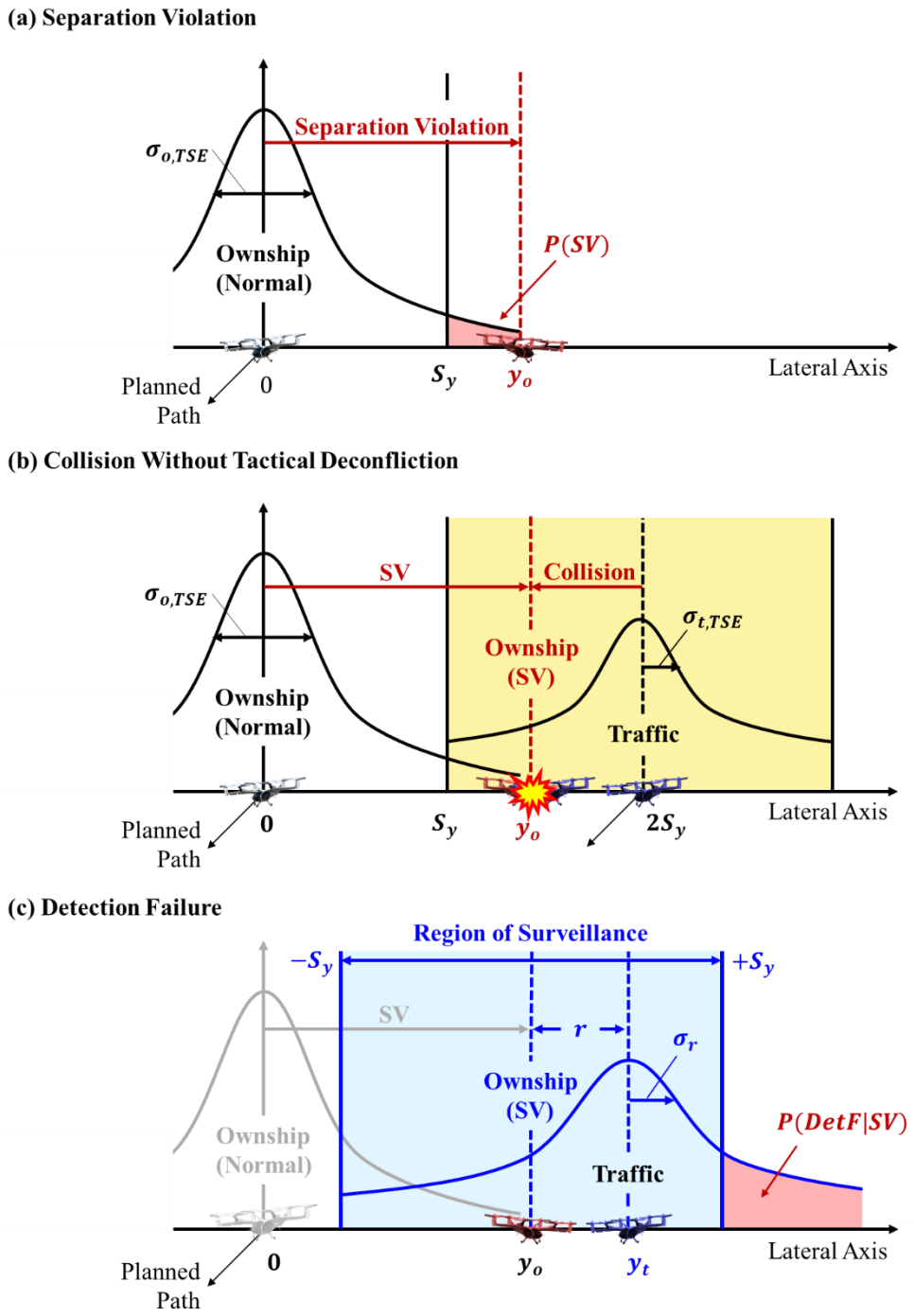

FIGURE 5 Illustration of Separation Violation, Collision Without Tactical Deconfliction, and Detection Failure. (Adapted, with permission, from [6] © IEEE proceedings).

B. Collision Risk Decomposition

In the presence of a detection system, a collision can occur only when three conditions are satisfied: an SV occurs, the conflicting traffic is not detected given the SV, and the resulting encounter leads to a collision [5, 6]. Figure 5 illustrates the events involved in this collision process. Accordingly, the collision risk can be decomposed into three terms: the probability of SV, the conditional probability of detection failure given SV, and the conditional probability of collision given both SV and detection failure [5, 6]. Under the operational assumptions described above, the collision probability in the presence of a detection system, denoted as $P(CO_{Det})$, is expressed as [6]:

$$P(CO_{Det}) = P(CO|DetF, SV) \cdot P(DetF|SV) \cdot P(SV), \tag{1}$$

where the involved events are defined as follows:

- **Separation Violation (SV)**: An event in which the ownship's true lateral position deviates from its planned path and exceeds the prescribed lateral SD.
- **Detection Failure (DetF)**: An event in which the estimated relative distance exceeds the SD even though the two aircraft are actually closer than the SD.
- **Collision (CO)**: An event in which two aircraft physically overlap.

On the other hand, the collision probability without a detection system, denoted as $P(CO_{NoDet})$, is decomposed as:

$$P(CO_{NoDet}) = P(CO|SV) \cdot P(SV). \tag{2}$$

This equation is used when the detection system is absent or unavailable due to malfunction. In this case, the collision probability depends only on the occurrence of an SV and the conditional probability that the SV results in a collision, because no risk reduction from the detection system is available.

C. Calculation of Probability Terms

As illustrated in Figure 5(a), the probability of SV is computed as [6]:

$$P(SV) = \int_{S_y}^{\infty} f_O\left(y; 0, \sigma_{o,TSE}^2\right) dy, \tag{3}$$

where $f(\cdot; \mu, \sigma^2)$ is a probability density function with mean μ and variance σ^2. Here, $f_O(\cdot)$ is the ownship TSE probability density function. The standard deviation $\sigma_{o,TSE}$ represents the standard deviation of the ownship TSE and is defined as the RSS of the NSE and FTE.

As illustrated in Figure 5(b), the joint probability of collision and SV without a detection system is expressed as [4]:

$$P(CO_{NoDet}) = P(CO|SV) \cdot P(SV) = 2\int_{S_y}^{3S_y} \int_{y_o - y_t - \lambda_y}^{y_o - y_t + \lambda_y} f_T\left(y_t\,; 2S_y, \sigma_{t,TSE}^2\right) \cdot f_O\left(y_o; 0, \sigma_{o,TSE}^2\right) dy_t\, dy_o, \tag{4}$$

where y_t is the true position of the traffic aircraft, $f_T(\cdot)$ is the traffic TSE probability density function, and λ_r is the lateral size of aircraft. The factor of two accounts for the number of aircraft involved in the collision. The inner integral bounds represent the range of ownship positions for which the two aircraft physically overlap, while the outer integral bounds correspond to the region in which the traffic aircraft can exist.

As illustrated in Figure 5(c), the joint probability associated with DetF and SV in the presence of a detection system is expressed as:

$$\begin{aligned} P(CO_{Det}) &= P(CO, DetF|SV) \cdot P(SV) \\ &= 2\int_{S_y}^{3S_y} \int_{y_o - y_t - \lambda_y}^{y_o - y_t + \lambda_y} f_T\left(y_t; 2S_y, \sigma_{t,TSE}^2\right) \cdot f_O\left(y_o; 0, \sigma_{o,TSE}^2\right) \cdot \left[1 - \Phi\left(S_y; y_t - y_o, \sigma_{Det}\right)\right] dy_t\, dy_o, \end{aligned} \tag{5}$$

where $\Phi\left(S_y; y_t - y_o, \sigma_{Det}\right)$ is the cumulative distribution function of the relative-distance distribution with mean $y_t - y_o$, which is the true relative distance after SV, and variance σ_{Det}^2. The variance σ_{Det}^2 represents the detection uncertainty. The integral bounds are the same as those in (4).

D. ADS-B-Based Modelling of Traffic TSE and Detection Uncertainty

A key contribution of this study is to represent both traffic-state uncertainty and detection uncertainty directly using ADS-B integrity information. For the traffic aircraft, the standard deviation of the ADS-B-based position error is modeled from ADS-B integrity information as:

$$\sigma_{t,ADSB} = \frac{R_{NIC}}{K_{SIL}}. \tag{6}$$

where R_{NIC} denotes the NIC containment radius and K_{SIL} is the Gaussian integrity multiplier corresponding to the reported SIL. Consistent with the ADS-B performance requirement adopted in this study, the SIL is taken as 3, which yields K_{SIL} of 5.33. Accordingly, the traffic-aircraft position uncertainty used in the collision model is defined as:

$$\sigma_{t,TSE} = \sqrt{\sigma_{t,ADSB}^2 + \sigma_{FTE}^2}. \tag{7}$$

For the detection model, the uncertainty in the estimated relative distance is represented by the RSS of the ownship and traffic ADS-B position uncertainties, given by:

$$\sigma_{Det} = \sqrt{\sigma_{o,ADSB}^2 + \sigma_{t,ADSB}^2}. \tag{8}$$

Because ADS-B integrity information is generally consistent under the same operating condition, we assume that the ownship and traffic ADS-B position uncertainties are identical, i.e., $\sigma_{o,ADSB} = \sigma_{t,ADSB}$. Under this assumption, the detection uncertainty is simplified as:

$$\sigma_{Det} = \sqrt{2} \cdot \sigma_{t,ADSB}. \tag{9}$$

This formulation establishes a direct relationship between standardized ADS-B integrity indicators and the uncertainty terms used in the safety risk assessment. As a result, variations in ADS-B integrity performance can be explicitly reflected in both the traffic TSE and the relative-distance distribution.

4.2 Failure Modelling

Another important aspect of the proposed framework is that it explicitly accounts for the identified failure conditions of all identified systems. In safety-critical UAM operations, system failures may substantially affect collision risk; therefore, failure conditions must be incorporated into the safety risk assessment in addition to nominal operation.

For the navigation system, a failure condition is modeled as an additional bias in the ownship TSE, as illustrated by the gray line in Figure 3. This is because a navigation-system failure shifts the estimated ownship position used for separation assessment and therefore changes the TSE distribution directly. The magnitude of the failure bias is determined using a methodology adopted in integrity risk analysis. When a navigation sensor is monitored by an integrity monitor, the corresponding undetected failure bias can be estimated [11]. A representative example is a residual-based receiver autonomous integrity monitor (RB-RAIM) within a Kalman-filter framework, for which the worst-case slope or minimum detectable error (MDE) method can be used to derive the failure bias [12-14]. In this study, the UAM platform is assumed to be equipped with integrity monitors for each navigation sensor, and the MDE approach is applied to determine the failure bias for each navigation-system failure condition.

For the detection system, a failure condition is modeled as a situation in which the detection system is unavailable. Under this condition, tactical deconfliction cannot be credited, and the collision risk is therefore evaluated using the collision model without detection in Equation (4) rather than the collision model with detection in Equation (5). This reflects the loss of surveillance capability in the tactical layer and provides a conservative treatment of detection-system failure conditions.

Accordingly, navigation-system failure conditions and detection-system failure conditions are represented through different mechanisms in the proposed framework: the former through a biased ownship TSE distribution, and the latter through the removal of tactical detection from the collision-risk calculation.

4.3 Final MSD Determination

The final MSD is determined by comparing the collision risk results over all identified operating conditions [4]. For a given UAM system configuration, the TLS is first allocated to each subsystem and its operating condition, including both nominal and failure conditions. Let the set of operating conditions be denoted by

$$H = \{Nom, GNSSF, INSF, ADSBF\} \tag{10}$$

where Nom denotes the nominal condition, and $GNSSF$, $INSF$, and ADSBF denote the GNSS, INS, and ADS-B failure conditions, respectively.

For each operating condition h, the collision probability is evaluated as a function of the lateral SD S_y as:

$$P_{CO,h}(S_y) = \begin{cases} P_{CO,Det,h}(S_y) & h \in \{Nom, GNSSF, INSF\}, \\ P_{CO,NoDet,h}(S_y) & h = ADSBF, \end{cases} \tag{11}$$

where $P_{CO,Det,h}(S_y)$ is computed using the collision model with detection in Equation (5), and $P_{CO,NoDet,h}(S_y)$ is computed using the collision model without detection in Equation (4). This distinction captures the different ways in which navigation-system and detection-system failure conditions affect collision risk.

The condition-specific MSD is then defined as:

$$MSD_h = min\{\, S_y \mid P_{CO,h}(S_y) \le TLS_h \,\}, \qquad h \in H, \tag{12}$$

where TLS_h is the TLS allocated to operating condition h. In practice, MSD_h is obtained by a one-dimensional search over S_y, starting from a sufficiently large SD and decreasing it until the minimum value satisfying $P_{CO,h}(S_y) \le TLS_h$ is found.

Finally, the final lateral MSD is determined as the maximum value among all operational conditions:

$$MSD = \max_{h \in H} MSD_h. \tag{13}$$

This definition ensures that the final MSD satisfies all allocated TLS requirements under the identified operating conditions. Equivalently, the resulting MSD guarantees TLS-level safety across all operational conditions.

5.0 Case Study

To validate the proposed methodology, a case study is conducted for a UAM system employing a GNSS/INS-integrated extended Kalman filter (EKF) for navigation and an ADS-B-based detection system. The proposed framework is applied to compute the MSD, and the resulting MSD is then analyzed with respect to changes in ADS-B integrity parameters and ownship navigation system configurations.

5.1 Simulation Parameters

The case study was conducted using the simulation parameters summarized in Table 2. The TLS was varied from 10^{-7} to 10^{-10}, and, for simplicity, the TLS was uniformly allocated to all operational conditions considered in the analysis. Although a more refined allocation strategy could be adopted, such optimization is left for future work. Accordingly, the condition-specific MSDs and the final MSD were evaluated under an equal TLS allocation.

For the ownship navigation system, the NSE was set to 25.02 m, which corresponds to the performance of a GNSS/INS-integrated EKF using GPS L1 C/A measurements and a consumer-grade inertial measurement unit (IMU) under urban-canyon conditions [15]. The FTE was set to 15 m based on the performance requirement defined in performance-based navigation (PBN) for operations below 1,500 m [16]. The standard deviation of the ownship TSE was then obtained as the RSS of the standard deviation of NSE and FTE, yielding 29.17 m. The prior probabilities of GNSS and INS failure conditions were each set to 10^{-4}. The aircraft size was set to 14.5 m based on the dimensions of the Joby S4 aircraft [17].

For navigation-system failure conditions, it was assumed that integrity monitors were available for each navigation sensor. Specifically, a Kalman filter (KF) residual-vector-based integrity monitor was assumed for GNSS, while a KF innovation-vector-based integrity monitor was assumed for INS. The magnitude of the undetected GNSS failure bias was determined using the method proposed in [12-13], and the corresponding INS failure bias was determined using the method proposed in [14].

The ADS-B parameters were selected to satisfy the performance requirements introduced earlier [10]. The NIC values were set to 8 and 9, which are commonly broadcast in practice, corresponding to containment radii of 185.2 m and 75 m, respectively. SIL was fixed at 3, for which the associated Gaussian integrity multiplier is 5.33. The SDA values were set to 2 and 3, corresponding to prior probabilities of ADS-B failure of 10^{-5} and 10^{-7}, respectively. Finally, using Equation (9), the resulting detection uncertainty values were 49.14 m and 19.90 m for NIC = 8 and 9, respectively. The following subsections use these parameters to compute the condition-specific MSDs and the final MSD.

TABLE 2
Simulation Parameters.

	Parameter	Value	
Ownship Parameter	Safety Requirement (TLS)	$10^{-7} – 10^{-10}$	
	Ownship NSE ($\sigma_{o,NSE}$)	25.02 m	
	Ownship FTE ($\sigma_{o,FTE}$)	15 m	
	Ownship TSE ($\sigma_{o,TSE}$)	29.17 m	
	Prior Probability (P_{GNSSF}, P_{INSF})	10^{-4}	
	Size of Aircraft (λ_y)	14.5 m	
	Integrity Monitor	GNSS	KF Residual-vector-based RAIM
		INS	KF Innovation-vector-based RAIM
ADS-B Parameter	Containment Radius (R_{NIC})	185.2 m, 75 m (NIC = 8, 9)	
	Gaussian Multiplier (K_{SIL})	5.33 (SIL = 3)	
	Prior Probability (P_{ADSBF})	10^{-5}, 10^{-7} (SDA = 2, 3)	
	Detection Uncertainty (σ_{Det})	49.14 m, 19.90 m	

5.2 Results

Figure 6 shows the condition-specific MSDs as functions of the TLS for two ADS-B containment radii: 185.2 m (left) and 75 m (right). The x-axis represents $\log_{10}$(TLS), and moving to the right corresponds to a more stringent safety requirement because the allowable fatal accident rate becomes smaller. The y-axis represents the minimum separation distance in meters. Each curve corresponds to the MSD associated with a specific operational condition, and the final MSD at a given TLS is determined by the largest value among those condition-specific MSDs.

Overall, Figure 6 shows that the required MSD increases as the TLS becomes more stringent. This trend is observed for all operational conditions because a stricter safety requirement requires a lower allowable collision risk, which in turn requires a larger separation distance. For the case with a containment radius of 185.2 m, the nominal condition yields the largest MSD over the entire TLS range considered. Therefore, the final MSD is determined by the nominal condition throughout this case. In particular, at a TLS of 10^{-9}, indicated by the red vertical line, the final MSD is 128 m, as marked by the red dot in the left panel.

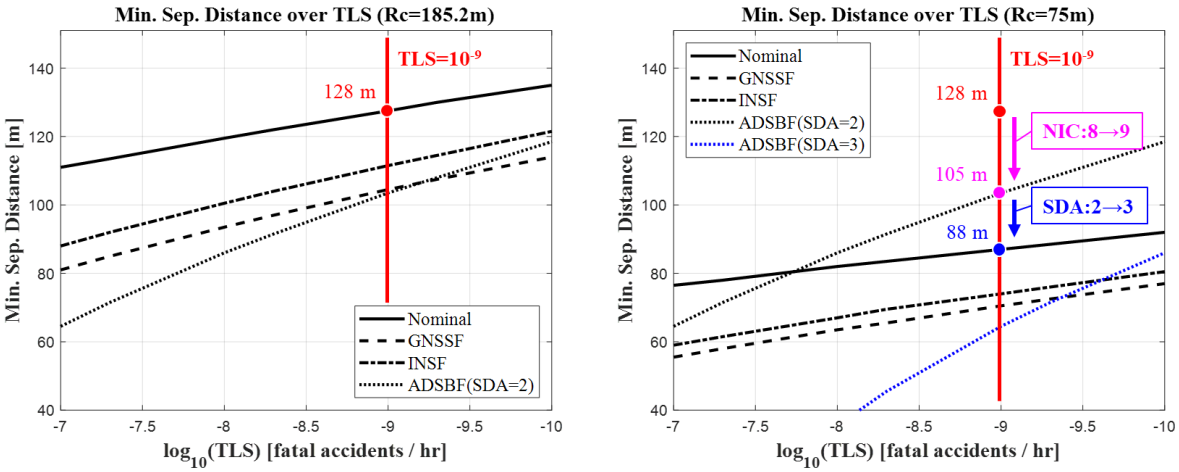

FIGURE 6 Condition-specific MSD as a function of TLS for containment radii of 185.2 m (left) and 75 m (right). The red vertical line indicates a TLS of 10^{-9} fatal accidents per hour, and the colored markers denote the corresponding final MSD values.

When the NIC is improved from 8 to 9, the containment radius decreases from 185.2 m to 75 m, and the resulting condition-specific MSDs are shown in the right panel. In this case, the nominal, GNSSF, and INSF curves all decrease. This reduction occurs because the improved ADS-B integrity information reduces the uncertainty in the traffic position estimate and improves detection capability, which lowers the collision risk for those operational conditions. By contrast, the ADSBF curve remains unchanged. This is because the ADS-B failure condition is evaluated using the collision model without detection, so the benefit of improved ADS-B integrity information cannot be credited once the detection system is assumed to be unavailable.

An important result in the right panel is that the governing operational condition changes with TLS. Up to approximately $10^{-7.7}$, the nominal condition still determines the final MSD. However, as the TLS becomes more stringent, the ADSBF condition becomes dominant and determines the final MSD. At a TLS of 10^{-9}, the final MSD becomes 105 m, as indicated by the magenta dot. This result shows that improving NIC alone can reduce the MSD, but the achievable reduction is limited when the ADS-B failure condition remains unchanged. In other words, even if nominal ADS-B accuracy and detection performance improve, the final separation requirement is eventually bounded by the collision risk associated with ADS-B unavailability under stringent TLS requirements.

To further reduce the impact of the ADS-B failure condition, SDA was improved from 2 to 3, which reduces the prior probability of ADS-B failure. This case is represented by the blue dotted curve in the right panel. As expected, the ADSBF curve decreases significantly when SDA is improved. As a result, the ADSBF curve falls below the nominal curve, and the final MSD is again determined by the nominal condition rather than the ADS-B failure condition. At a TLS of 10^{-9}, the corresponding final MSD is approximately 88 m, as indicated by the blue dot.

These results quantify how much the final MSD can be reduced through improvements in ADS-B integrity parameters. More importantly, they show that the effectiveness of ADS-B performance enhancement depends not only on nominal surveillance accuracy but also on the probability of ADS-B failure. Therefore, both nominal ADS-B integrity and failure condition performance should be considered together when evaluating separation requirements for safety-critical UAM operations.

5.3 Sensitivity Analysis

Figure 7 presents the sensitivity of the final MSD to the ownship navigation system configuration. In this analysis, SDA was fixed at 2. The left panel shows the results for a containment radius of 185.2 m, while the right panel shows the results for a containment radius of 75 m. The four curves correspond to the following navigation configurations [15]: GPS L1 with a consumer-grade IMU, GPS L1 with a tactical-grade IMU, GPS L1 + Galileo E1 with a consumer-grade IMU, and GPS L1/L2 + Galileo E1/E2 with a consumer-grade IMU. The corresponding NSE values are 25.02 m, 5.15 m, 17.84 m, and 10.70 m, respectively.

Overall, the results show a clear tendency for the final MSD to decrease as the performance of the ownship navigation system improves. This trend is observed for both containment radii. Among the configurations considered, GPS L1/L2 + Galileo E1/E2 with a consumer-grade IMU, referred to here as the dual-frequency multi-constellation configuration (DFMC), yields the smallest MSD over the entire TLS range, indicating that it is the most effective option for reducing separation requirements.

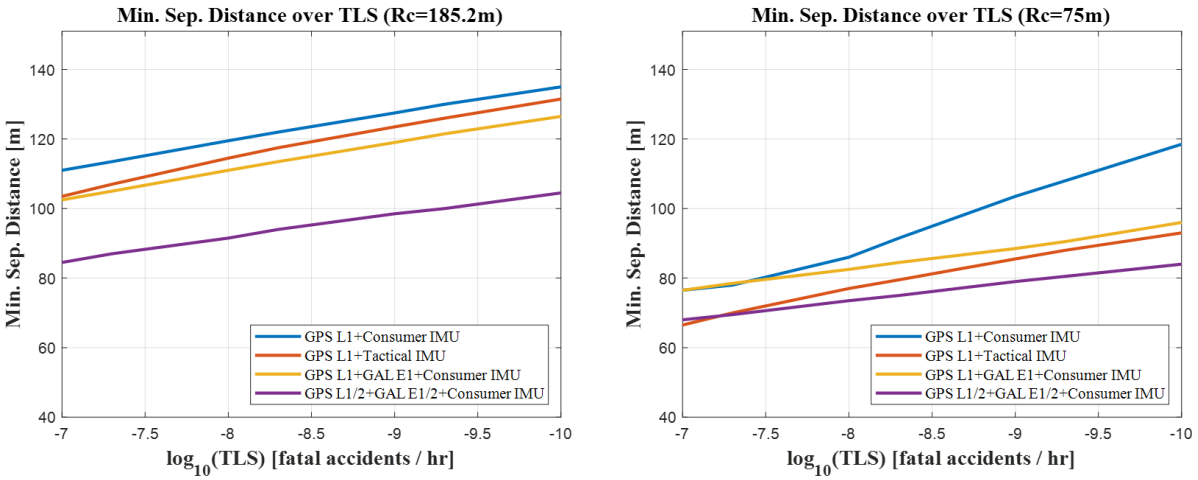

FIGURE 7 Final MSD as a function of TLS for different ownship navigation system configurations with SDA = 2. The left panel corresponds to a containment radius of 185.2 m, and the right panel corresponds to a containment radius of 75 m. The four curves represent GPS L1 with a consumer-grade IMU, GPS L1 with a tactical-grade IMU, GPS L1 + Galileo E1 with a consumer-grade IMU, and GPS L1/L2 + Galileo E1/E2 with a consumer-grade IMU, respectively.

This result can be explained by two effects. First, as the number and quality of GNSS measurements increase, the ownship NSE improves owing to better measurement availability and geometry. Second, improved navigation observability enhances the detectability of GNSS and INS failure conditions, thereby reducing the magnitude of the undetected failure biases used in the failure condition analysis. As a result, both nominal navigation uncertainty and failure condition risk are reduced, leading to a smaller final MSD.

These results indicate that improving the ownship navigation system is an effective means of reducing separation requirements while maintaining the required level of safety. In particular, the DFMC appears to be the most promising among the configurations considered for enabling reduced separation in future high-density UAM operations.

6.0 Conclusion

In urban air mobility (UAM) operations, constrained airspace, stringent safety requirements, and limited operational data continue to make the determination of safe yet efficient separation distances a challenging problem. To address this issue, our prior research introduced the concept of the minimum separation distance (MSD) and proposed a safety risk assessment (SRA) framework with reduced reliance on extensive flight data. Building on this foundation, the present study extended the framework in two important ways. First, the generic surrogate detection model used in the earlier proceeding was replaced with an ADS-B-based representation, in which the traffic-state uncertainty and detection uncertainty are modeled directly from ADS-B integrity information, particularly NIC, SIL, and SDA. Second, the framework was extended beyond nominal operation by explicitly accounting for identified failure conditions in both the navigation system and the detection system. Through these extensions, the proposed methodology provides a more traceable and operationally meaningful framework for determining the lateral MSD for UAM tactical deconfliction.

The proposed methodology was applied to a case study involving a UAM system equipped with a GNSS/INS-integrated extended Kalman filter navigation system and an ADS-B-based detection system. The case study evaluated the condition-specific MSDs and the final MSD, and further examined their sensitivity to ADS-B integrity parameters and ownship navigation system configurations. The results showed that improving ADS-B integrity can substantially reduce the required separation distance. In particular, when NIC was improved from 8 to 9 and SDA was improved from 2 to 3, the final MSD decreased from 128 m to 88 m at a TLS of 10^{-9}, achieving up to a 31% reduction in MSD. In addition, the sensitivity analysis of ownship navigation system configurations showed that the dual frequency multi constellation configuration yielded the smallest MSD among the configurations considered, indicating that it is the most effective for reducing separation requirements while maintaining the required level of safety. The methodology developed through this study is expected to provide a practical framework for UAM stakeholders to assess separation requirements, evaluate the benefit of ADS-B integrity improvements, and identify effective navigation-system configurations, particularly during the early stages of high-density UAM deployment.

ACKNOWLEDGMENTS

This work was supported by the National Research Foundation of Korea (NRF) grant funded by the Korea government (MSIT) (No. RS-2025-02213804) and the NRF grant funded by the Korea government (MSIT) (No. RS-2024-00354326).

REFERENCES

[1] NASA (2021). UAM Vision Concept of Operations (ConOps) UAM Maturity Level (UML) 4 Version 1.0.

[2] Federal Aviation Administration (2019). Authorization of Aircraft and Operators for Flight in Reduced Vertical Separation Minimum (RVSM) Airspace.

[3] Chen, C., et al. (2019). Defining Well Clear Separation for Unmanned Aircraft Systems Operating with Noncooperative Aircraft. AIAA Aviation 2019 Forum.

[4] Kim, J., Nam, G., Min, D., Kim, N.M., & Lee, J. (2023). Safety Risk Assessment Based Minimum Separation Boundary for UAM Operations. 2023 IEEE/AIAA 42nd Digital Avionics Systems Conference (DASC).

[5] Kim, J., Nam, G., Kim, N. M., Min, D., Kim, N.M., & Lee, J. (2024). Determining Minimum Separation Boundary for UAM Tactical Deconfliction. Proceedings of the ION 2024 Pacific PNT Meeting.

[6] Kim, J., Nam, G., Min, D., Kim, N.M., Lee, J. & Pullen, S. (2024). Minimum Separation Boundary for UAM Tactical Deconfliction Based on Avoidance Risk Ratio Model. 2024 IEEE/AIAA 43rd Digital Avionics Systems Conference (DASC).

[7] Federal Aviation Administration. (2022). Automatic Dependent Surveillance-Broadcast Operations (Advisory Circular No. 90-114B, Change 1). U.S. Department of Transportation.

[8] Manfredi, G., & Jestin, Y. (2018). Are You Clear About 'Well Clear'?. 2018 International Conference on Unmanned Aircraft Systems (ICUAS).

[9] Johnson, M., & Larrow, J. (2020). UAS traffic management conflict management model.

[10] Federal Aviation Administration. (2026). Automatic Dependent Surveillance-Broadcast (ADS-B) Out equipment performance requirements. 14 CFR § 91.227. Electronic Code of Federal Regulations.

[11] Lee, J., Kim, M., Min, D. & Lee, J. (2019). Integrity Algorithm to Protect against Sensor Faults in Tightly-coupled KF State Prediction. Proceedings of the 32nd International Technical Meeting of The Satellite Division of the Institute of Navigation (ION GNSS+ 2019).

[12] Tanıl, Ç., Khanafseh, S., Joerger, M. & Pervan, B. (2018). An INS Monitor to Detect GNSS Spoofers Capable of Tracking Vehicle Position. IEEE Transactions on Aerospace and Electronic Systems, 54(1), 131–143.

[13] Joerger, M. & Pervan, B. (2013). Kalman Filter-Based Integrity Monitoring Against Sensor Faults. Journal of Guidance, Control, and Dynamics, 36(2), 349–361.

[14] Lee, J., Kim, M., Lee, J. & Pullen, S. (2018). Integrity assurance of Kalman-filter based GNSS/IMU integrated systems against IMU faults for UAV applications. Proceedings of the 31st International Technical Meeting of The Satellite Division of the Institute of Navigation (ION GNSS+ 2018).

[15] Groves, P. D. (2013). Principles of GNSS, Inertial, and Multi-Sensor Integrated Navigation Systems.

[16] ICAO (2008). Performance based Navigation (PBN) Manual. ICAO Doc 9613 AN/937, 3rd Edition.

[17] Zahn, D. & Ringelberg, W. (2023). Urban Air Mobility (UAM) Procedure Design and Flight Test Evaluation Methodology. Society of Experimental Test Pilots (SETP) Symposium 2023.